



Swansea University
Prifysgol Abertawe



Cronfa - Swansea University Open Access Repository

This is an author produced version of a paper published in :
International Journal of Fatigue

Cronfa URL for this paper:

<http://cronfa.swan.ac.uk/Record/cronfa5833>

Paper:

Whittaker, M. (2011). Considerations in fatigue lifing of stress concentrations in textured titanium 6-4. *International Journal of Fatigue*

<http://dx.doi.org/10.1016/j.ijfatigue.2011.05.001>

This article is brought to you by Swansea University. Any person downloading material is agreeing to abide by the terms of the repository licence. Authors are personally responsible for adhering to publisher restrictions or conditions. When uploading content they are required to comply with their publisher agreement and the SHERPA RoMEO database to judge whether or not it is copyright safe to add this version of the paper to this repository.

<http://www.swansea.ac.uk/iss/researchsupport/cronfa-support/>

Considerations in fatigue lifing of stress concentrations in textured titanium alloys

M.T. Whittaker

*Materials Research Centre
School of Engineering, Swansea University
Singleton Park, Swansea SA2 8PP*

Abstract

The effect of crystallographic texture has been considered in attempting to derive a total life prediction capability for the titanium alloy Ti6-4. Orientation effects due to texture are shown to be a result of stress relaxation in strain control specimens, and consequently occur in some cases of notched specimens. It is shown that these effects can be predicted using analytical methods such as the Modified Coffin-Manson and Walker strain approaches. Additional failure mechanisms such as cold dwell prohibit accurate predictions at higher R ratios. It is also acknowledged that texture effects can occur in the crack propagation phase of notched specimens and should be considered in a total life model.

1. Introduction

In the half century since the introduction of titanium alloys into the aero industry considerable advances have been made, particularly through improved compositions and a better understanding of the processing methods used on those alloys. A great deal of research has been undertaken on understanding the impact of microstructural features arising from these processing methods. Crystallographic texture is one of these features. It was originally seen as having a detrimental effect on mechanical response, however, the harnessing of texture could be important to continue the advance of alloy capability for specific applications. It is believed that provided the effects of texture are well understood then it should be possible to match the best properties from the textured material with the most demanding loading directions.

Previous work [1-4] has shown the type of variations possible in monotonic tensile, axial-fatigue and torsion-fatigue tests due to texture. However, engineering applications of these alloys are rarely simple and stress raising features caused by geometrical discontinuities are common, along with more complex stress states. In a laboratory environment both of these issues can be examined through the strategic use of notched specimens. Limited data is available on the effects of texture on notched specimens [5] and no consideration has been given the further complication of varying the R ratio.

Traditional approaches to fatigue lifing of notched specimens involve the production of strain control data as a basic input. It is argued that material in the plastic region at the notch root undergoes an essentially strain control form of cyclic deformation [6] and as such plain specimen strain control data can be applied in a number of ways to predict crack initiation lives. Previous work [7,8] has shown that under certain circumstances in titanium alloys, both the Coffin-Manson and Walker strain approaches to notched life prediction can be successful. The ability of the methods

to cope with the mechanical anisotropy brought about by texture however, has not been previously considered.

The current research formed part of a larger programme of work which investigated both the production of textures in titanium alloys and the mechanical anisotropy which results from them. However, whilst the current publication makes mention of these texture development issues, the focus is on the mechanical test results. For more detailed discussions the reader is directed to other published literature [9].

2. Experimental methods

The research programme focused on the $\alpha+\beta$ titanium alloy, Ti-6Al-4V (Ti6-4). The alloy was supplied in plate form with a plate thickness of 0.55' (14mm), having been processed by unidirectional rolling in the $\alpha+\beta$ temperature regime, with the material subsequently air cooled. Following processing the microstructure consisted of nearly equiaxed primary alpha grains as part of a bimodal structure. Deviation from equiaxality was evident as slight elongation of the grains in the final rolling direction. The average grain size was of the order of $15\mu\text{m}$, Figure 1 (a). The crystallographic texture following processing is shown in Figure 1 (c). The texture is completely described by the three orthogonal pole figures (0001) , $(11\bar{2}0)$, $(10\bar{1}0)$, Figure 1 (b). The material shows a classic basal/transverse texture with a peak texture intensity of x3 random. Although this is not a strong texture, it has been shown that due to the high primary alpha content, significant anisotropy is still observed [4].

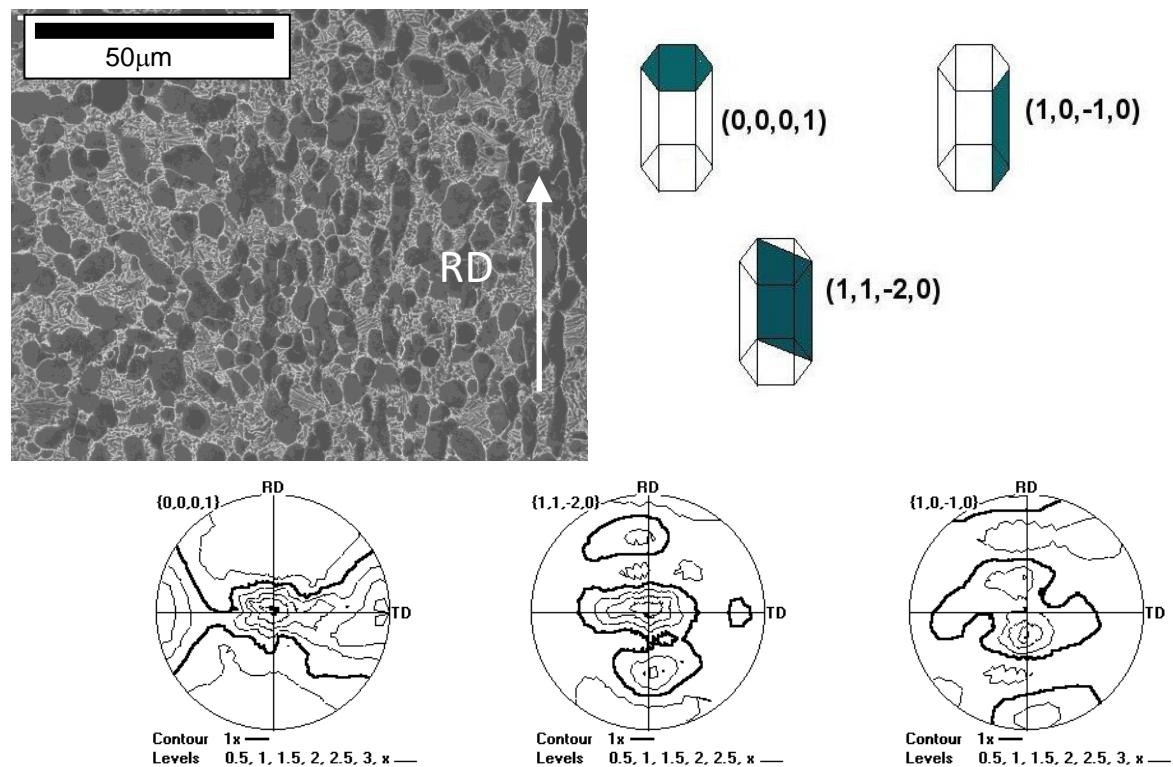


Figure 1: Microstructure and texture of Ti6-4. A bimodal structure with a basal transverse texture is observed.

Strain control testing was performed at room temperature using plain cylindrical specimens of 6mm diameter in accordance with BS7270 [10]. The test was controlled by an MTS extensometer with a gauge length of 10mm, and hysteresis loops were recorded using an in-house data logging system. Testing was conducted on specimens aligned at 0° (RD) and 90° (TD) to the rolling direction. Strain R ratios of -1 and 0 were employed, along with a trapezoidal 1-1-1-1 waveform (i.e. 1 sec hold at peak and minimum strain, with a 1 sec ramp).

Notch tests were undertaken under load control, at various stress R ratios including -1, 0 and 0.8 using a 5Hz sine waveform. The design of the V-cylindrical notch (VCN, $K_t=2.8$) and round cylindrical notch (RCN, $K_t=1.4$) specimens are shown in Figure 2.

Crack propagation tests were performed using an stress R ratio of 0.1 and a trapezoidal 1-1-1-1 waveform.

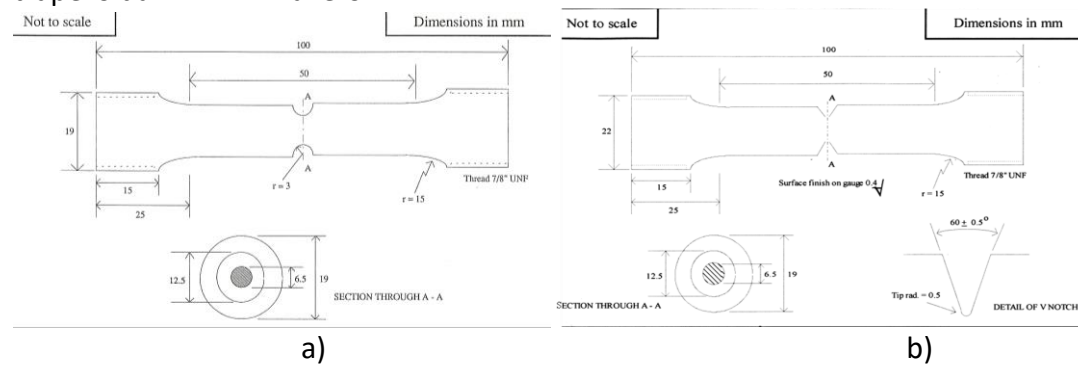


Figure 2: Specimen geometry of a) RCN ($K_t=1.4$) b) VCN ($K_t=2.8$)

The Coffin-Manson approach [11,12] to life prediction requires the applied strain for $R = -1$ strain control data to be partitioned into its elastic and plastic components, i.e.

$$\Delta \epsilon_{Tot} = C_e N_f^{\alpha 2} + C_p N_f^{\alpha 1} \quad (1)$$

Application of eqn (1) in the prediction of notch behaviour requires the strain range at the notch root to be determined. In the case of applied stresses which cause yielding at the notch root, typically in tests with a zero or positive R ratio, it is clearly desirable to calculate the evolution of stress and strain at the notch root by finite element methods. However, previous work [8] has shown that an acceptable approximation is given by Neuber's rule [13]

$$\text{Stress} \times \text{Strain} = \text{constant} \quad (2)$$

from which the peak and minimum stresses for cyclic loading can be determined. A more detailed analysis of this technique can be found elsewhere [8]

For $R = -1$ notches, the situation is simpler, since the applied peak elastic stresses are approximately equal to or lower than the yield stress of the material, so purely elastic behaviour can be assumed.

The Walker strain relationship is an empirical method for correlating R values [14]. The approach involves correlating strain control data of different R ratios using the expression

$$\Delta \varepsilon_w = \frac{\sigma_{\max}}{E} \left(\frac{\Delta \varepsilon E}{\sigma_{\max}} \right)^m \quad (3)$$

where; $\Delta \varepsilon_w$ = Walker strain

σ_{\max} = maximum stabilised stress

E = Modulus

$\Delta \varepsilon$ = strain range

m = Walker exponent

3. Results

As part of a wider programme of work, the production of rolled titanium plate has been simulated through the use of plane strain compression at temperatures ranging from 850-1150°C. Smith [9] indicates that PSC is indeed a valid tool for simulating the rolling process. Comparisons with the microstructure of the current material, Figure 1, are extremely favourable with work carried out at 950°C, similar to processing temperatures for the rolled plate. This type of $\alpha+\beta$ processing temperature can be seen to develop a bimodal microstructure with primary alpha grains of approximate diameter 15 μ m, interspersed with very fine transformed product. This type of microstructure has been shown to give extremely favourable fatigue performance [15,16]. The work by Smith also includes extensive pole figures regarding the development of texture in the material. It is useful to note that the pole figure intensities in the current material show similar values to those found by Smith at 950°C. The rolled plate had a more complex processing route (considered proprietary) than could be simulated by PSC however, and as such a basal/transverse rather than strong transverse texture is developed.

Previous work [4] has demonstrated that in this alloy significant texture effects can be seen under strain control loading. Figure 3 shows a comparison of strain control data for R = 0 and R = -1 loading conditions, for rolling direction (RD) and transverse direction (TD) specimens from the rolled plate. It is evident that there is little difference between RD and TD specimens for R = -1 loading, whereas for R = 0 loading the RD specimens show significantly longer fatigue lives on a strain range basis. The reason for the difference between RD and TD specimens for R = 0 tests has been shown to be related to the availability of slip in either orientation [4], Figure 4. In TD specimens prismatic slip, which is usually related to stress relaxation due to its lower critical resolved shear stress value, is not favoured due to the material texture. However, in RD specimens slip is easier, and combined with a lower modulus in this orientation, leads to a lower applied stress range, subsequently leading to a longer fatigue life. These orientation effects are not seen in R = -1 tests, since the applied strains for LCF behaviour do not lead to yielding in the material. Hence, the

differences in slip behaviour play no role, and there is no difference in the fatigue lives of the material. Figure 5 further illustrates the effect of stress relaxation in these strain control tests by considering only the effect of the stabilised stress range of these tests on the fatigue life. The y-axis has been normalized to remove the effect of increased modulus and UTS in the TD specimens brought about by an increased density of basal planes perpendicular to the loading direction in this orientation. This then illustrates that there is essentially no orientation effect purely as a function of stress, and that the controlling factor giving the orientation effect is the stress relaxation during the early strain control cycles, and the increased modulus of the TD specimens.

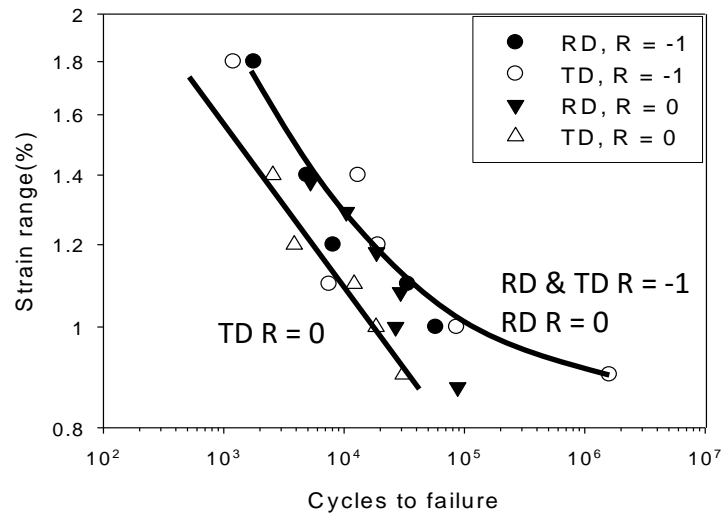


Figure 3: Comparison of strain control data in RD & TD specimens indicating a significant orientation effect for R=0 loading.

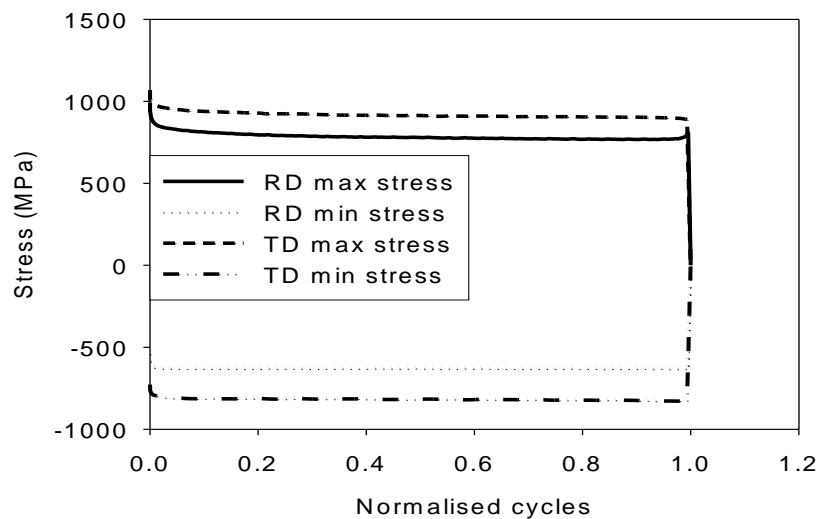


Figure 4: Stress plots for RD & TD specimens for a peak strain of 1.4%, R=0. It can be seen that the TD specimen operates over a larger stress range.

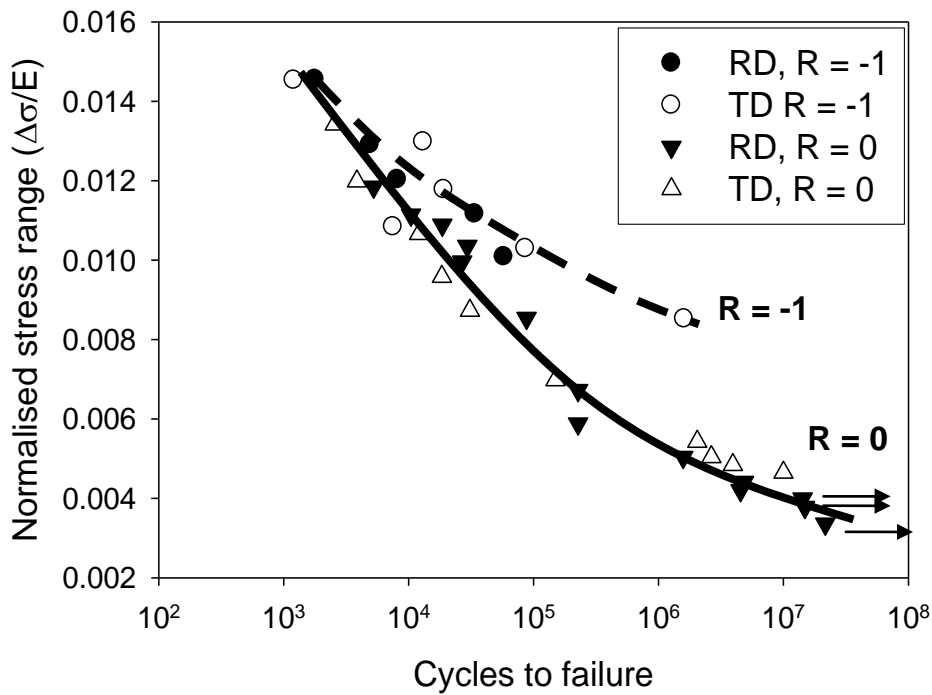


Figure 5: Modulus normalised stress range vs life for RD & TD specimens. It can be seen that when considered on this basis the orientation effect disappears.

As previously indicated [17] no orientation effect appears to exist in the RCN specimens. However, Figure 6 indicates that this is no longer the case when the stress concentration is increased, as in the VCN specimens. It is clear that there is now a significant effect of orientation in both R = 0 and R = -1 specimens.

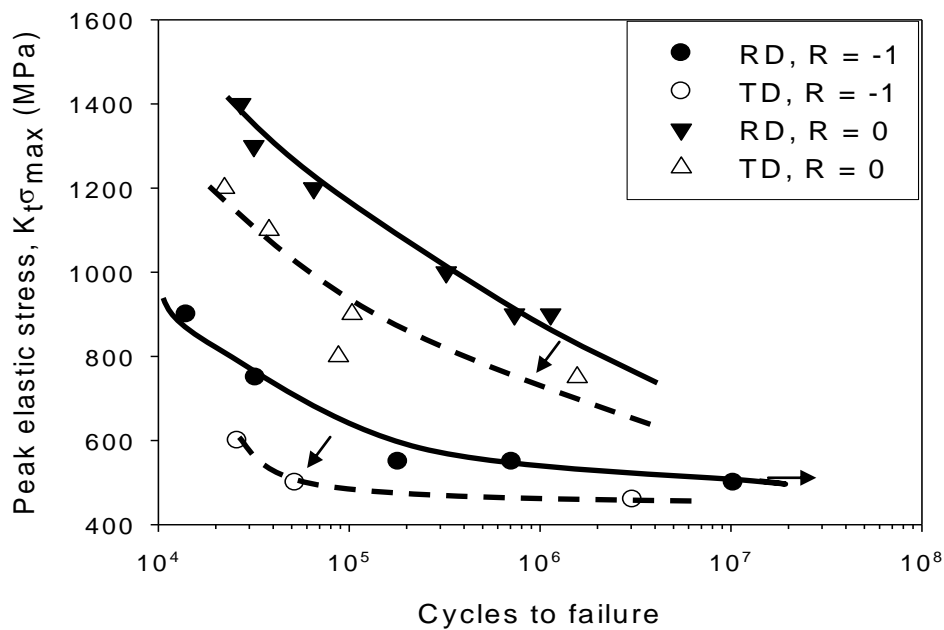


Fig 6: Orientation effects in VCN specimens. The effect can be seen in both R = 0 and R = -1 specimens.

3.1 Notched life predictions

As described earlier, there are many methodologies available for making predictions of notched specimen behaviour based on strain control data. The Coffin-Manson method however is one of the best known, and simplest to utilize. In the case of the RD specimens, partitioning of the data into its elastic and plastic components allowed for the constants to be defined as follows

C_e (Elastic constant)	0.0319
C_p (Plastic constant)	0.211
α_1 (Plastic exponent)	-0.599
α_2 (Elastic exponent)	-0.105

Table 1: Definition of constants for Coffin-Manson equation in RD specimens

In its simplest form however, the method is limited, in that it is ineffective in predicting the behaviour of notched specimens with significant mean stresses. A mean stress correction however can be applied, and reasonable results can be achieved through use of this Modified Coffin-Manson approach as shown in Figure 7.

$$\Delta \varepsilon_t = (\varepsilon_f - \varepsilon_m) N_f^{\alpha_1} + C_e (1 - \sigma_m / \sigma_{TS}) N_f^{\alpha_2}$$

where: ε_f is the fatigue ductility coefficient

ε_m is the mean strain

σ_m is the mean strain

σ_{TS} is the tensile strength

An alternative approach is the Walker strain technique, an empirical method for correlating R values. Each method offers its own benefits, although experience indicates that the Walker strain method is slightly more robust when mean stresses are introduced, although consequently the Coffin-Manson approach provides better results for fully reversed loading.

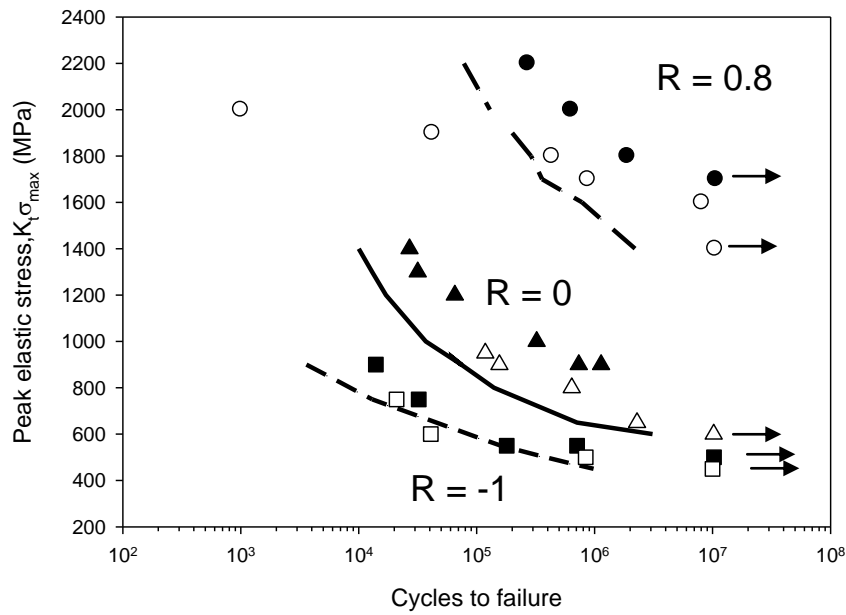


Figure 7: Modified Coffin-Manson predictions of VCN and RCN RD specimen fatigue lives. Lines indicate the predictions, solid black symbols indicate VCN specimens and clear white symbols indicate RCN specimens.

For the RD specimens, the exponent (m) in the Walker strain method was optimised at 0.5, meaning that the best fit expression took the form

$$\Delta \varepsilon_W = 0.00286 N_f^{-0.1225} \quad (4)$$

Figure 8 shows the results of the Walker strain approach, and it can be seen that accurate predictions are made for low R ratios. It should be noted that this type of prediction provides only an estimate of the crack initiation life in a notched specimen. The predictions are based on strain control data, and in these specimens, when a crack forms it propagates rapidly to failure. In a notched specimen, the crack travels through material experiencing stresses considerably lower than the notch root. Consequently a significant propagation phase should be considered for the notched specimen. Previous work [15] has shown through PD monitoring of titanium specimens that crack initiation often occurs at approximately 50% of the total life of the specimen. Assuming a propagation phase of approximately 50% in the notch specimens results in accurate life predictions.

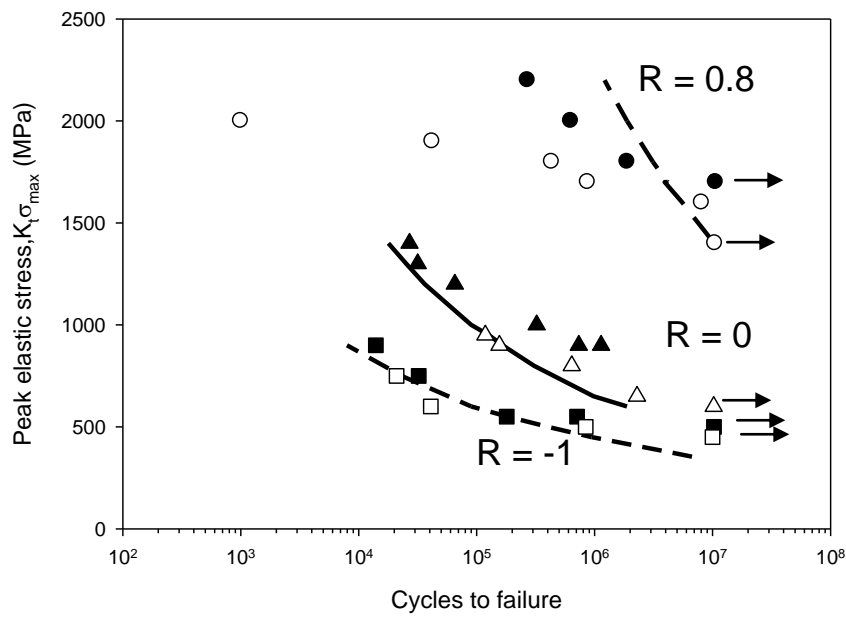


Figure 8: Walker strain predictions of VCN and RCN RD specimen fatigue lives. Lines indicate the predictions, solid black symbols indicate VCN specimens and clear white symbols indicate RCN specimens.

Attempts have been made to make predictions of TD notched specimen lives using both methods. In the case of the Modified Coffin-Manson approach, the constants were determined to be

C_e (Elastic constant)	0.0245
C_p (Plastic constant)	0.144
α_1 (Plastic exponent)	-0.500
α_2 (Elastic exponent)	-0.075

Table 2: Definition of constants for Coffin-Manson equation in TD specimens

and for the Walker strain method the best fit expression, with $m=0.3$, took the form

$$\Delta \varepsilon_W = 0.0161 N_f^{-0.0756} \quad (5)$$

In both cases predictions tended to be less accurate than for the RD specimens. Evidence of this is shown in Figure 9 where it can be seen that the predictions made by the Walker strain method overpredict the notched specimen lives, even without considering a crack propagation period.

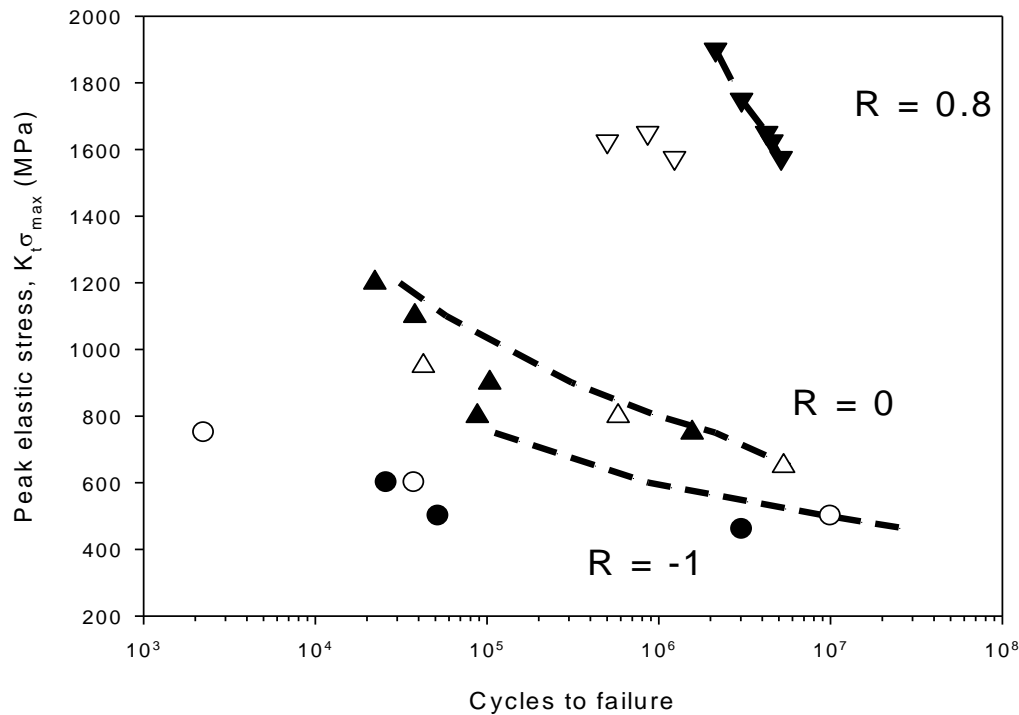


Figure 9: Walker strain predictions of VCN and RCN TD specimen fatigue lives. Lines indicate the predictions, solid black symbols indicate VCN specimens and clear white symbols indicate RCN specimens.

4. Discussion

Immediately apparent from Figure 7 is the fact that the sharper notched specimens (VCN) show a longer fatigue life than the RCN specimens. This is not unusual and is usually attributed to ‘weak link theory’. The VCN specimen has a lower volume of critically or near critically stressed material than the RCN specimen [17]. Since fatigue is probabilistic in nature, the larger the critically stressed volume, the larger the likelihood of one of these weak links being present and initiating the fatigue process. Hence RCN specimens statistically are always likely to fail at shorter lives. Interestingly, the VCN specimens show a strong dependence on orientation. This is in direct contradiction to previous work [18] which showed that for RCN specimens, no orientation effect occurred. It is useful to compare these findings with the results shown for the strain control specimens, Figures 3 & 5. The strain control data shows that RD specimens tend to show a significantly longer fatigue life than TD specimens, mainly due to the stress relaxation in the early part of the test and the increased modulus of the TD specimens, as explained previously. It appears that the VCN specimens show exactly the same trend. This perhaps, is not unexpected since the premise of the notch prediction work is that material at the notch root will experience a ‘strain control’ type of deformation because of its confinement by other lower stressed material. This however, does not explain why the RCN notch does not show an orientation effect.

It is likely that the conditions experienced at the notch root of the RCN specimen differ significantly from the VCN. The stress gradient away from the notch root is far more shallow in the RCN specimen because of the specimen geometry. The material at the notch root therefore is not confined to the same extent as in the VCN specimen, and the deformation is more akin to that of pure load control. It is therefore interesting to compare these results to the strain controlled specimens, plotted on a stabilised stress basis, Figure 5. It can be seen that on a pure stress range basis, no orientation effect exists, and hence the RCN specimens do not show an orientation effect. It should also be noted that the orientation effect is now seen in $R = -1$ VCN tests as well as $R = 0$, because of the higher applied stresses resulting in yield at the notch root.

It is clear that whichever prediction method is used, whilst good predictions are generally achieved for low R ratio tests, there are significant problems in making accurate predictions about $R = 0.8$ tests. The Walker strain method, Figure 8, does not achieve an accurate gradient, and the Modified Coffin-Manson method experiences similar problems, particularly with RCN specimens, although VCN predictions are reasonable. It has long been acknowledged [19-23] that titanium alloys are susceptible to strain accumulation at high mean stresses at low temperatures. This effect, loosely termed 'cold dwell' has been well documented across a number of near α and $\alpha+\beta$ titanium alloys including Ti6-4 [6]. This effect is usually characterised by the formation of 'quasi-cleavage facets', a mechanism for the formation of which has been proposed by Evans and Bache [21]. Fractographic analysis of the current specimens has shown evidence of these features, as can be seen in Figure 10.

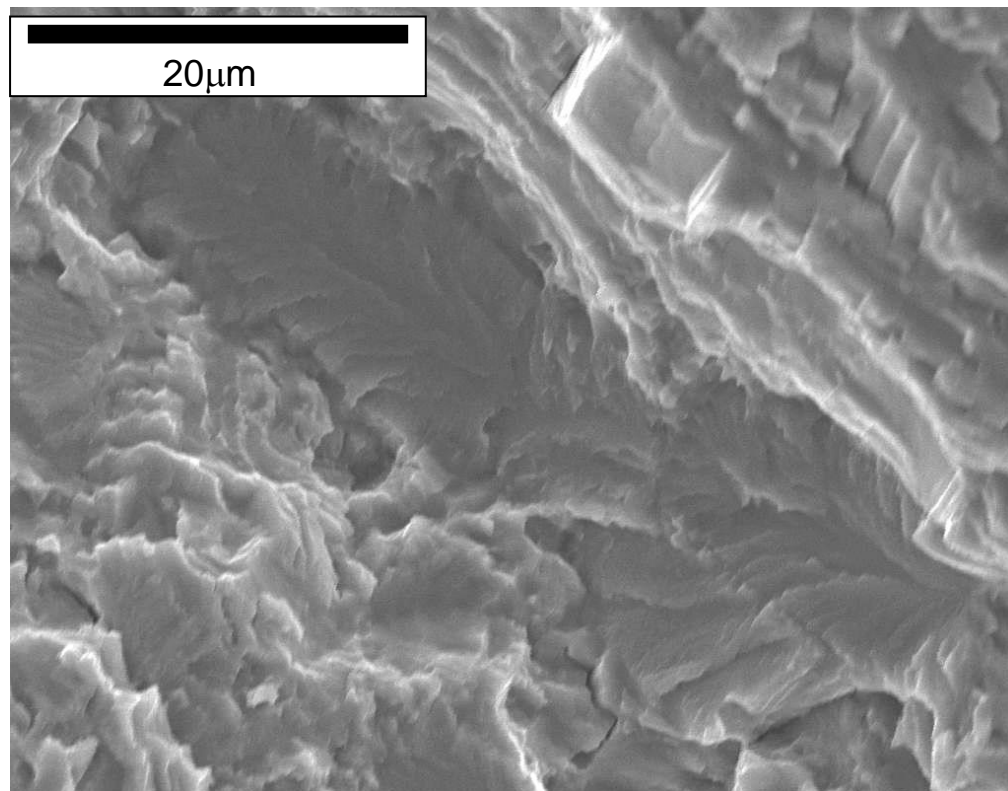


Figure 10: Quasi-cleavage facets in $R=0.8$ RCN specimen ($\sigma=1800\text{MPa}$, $N_f=433000$)

The density of these features was found to be increased in RCN specimens over VCN specimens, and also in TD specimens. These facets are usually formed because of stress redistribution from so called 'soft' (suitably orientated for slip) grains onto 'hard' grains (unsuitably orientated for slip). The hard grains will normally have basal planes orientated perpendicular to the loading direction, and it is clear from the pole figures in Figure 1 that there is an increased density of basal planes with this orientation in the TD specimens. Because of the shallow stress gradient associated with the RCN specimen, more material in this specimen is highly stressed, and hence facets tend to form more extensively. Ongoing research at Swansea University in fact shows that more accurate predictions can be made through considering these high R ratio tests in terms of the creep deformation rather than fatigue. Such an analysis results in a far shallower curve, which is more akin to the R=0.8 curves seen in Figures 7 & 8, and more similar in fact to a stress rupture curve for Ti6-4 at 20°C.

Predictions of TD specimens proved to be more challenging than RD specimens. Figure 9 indicates that predictions made using the Walker strain method tended to overpredict tested specimen lives. Similar problems were encountered using the Modified Coffin-Manson technique. Predictions of R = 0 and R = 0.8 tests may seem reasonable, but as described earlier, a significant crack propagation phase has yet to be added to these predictions. The reason for these overpredictions is most likely due to the fact that stress relaxation is difficult in the TD specimens as shown in Figure 4. Further restrictions are imposed by the triaxial stress at the root of the notch, leading to a high applied stress range, and hence shorter fatigue lives than predicted based on the strain control data.

Clearly in the development of a total life prediction capability, the crack propagation phase of specimens needs to be considered. In fact, more recently designers may work towards a 'life to first crack' philosophy in critical parts, where detection intervals will be based around an allowable number of cycles, between which a detectable crack would not propagate to failure. As such there is clearly a requirement for high quality crack propagation data. In the current work, it is useful to analyse whether there is an orientation effect on the crack propagation rate which needs to be considered for total life prediction.

Figure 11 compares crack propagation rates of specimens tested in RD & TD orientations. It can be seen that higher rates are experienced in the TD specimens, although it should be noted that this difference is minimal, especially when scatter between tests is considered. Bowen [24] found that values of the Paris exponent, m , were highest for the specimens growing in the $\langle 0001 \rangle$ direction along the (10-10) planes, with lowest m values for specimens growing in the $\langle 10-10 \rangle$ direction along the (-12-10) planes. The current work does not seem to correlate directly with these findings, although this is most likely due an extremely limited number of (10-10) prismatic planes suitably orientated in either the RD or TD orientations. However it should be noted that the material tested by Bowen was a highly transverse textured alloy, and the basal/transverse nature of the current material may be more difficult to derive clear trends from. The results however do show a strong correlation with the work by Peters et al [25]. Peters also found very little variation between RD and TD orientations for a basal/transverse texture. As such, for the current alloy no

significant difference in crack propagation life would be expected, although care should be taken as this may not be the case with other textured alloys.

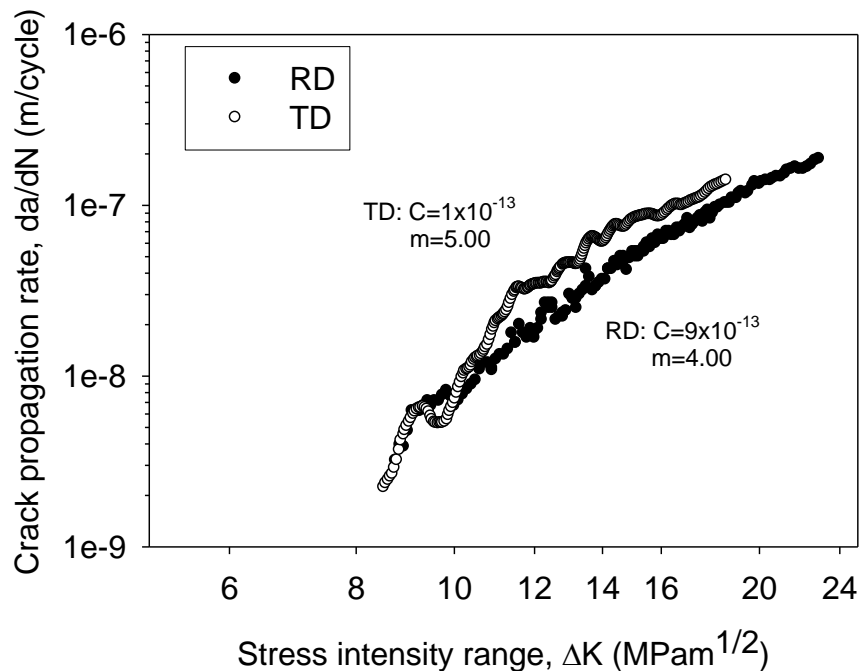


Figure 11: Crack propagation rates in RD & TD specimens, indicating a faster rate in TD specimens. Tests performed at R=0.1, 400MPa, trapezoidal 1-1-1-1 waveform. C and m are parameters calculated from the Paris equation.

5. Conclusions

The following conclusions can be drawn regarding the fatigue lifing of stress concentrations in this textured titanium alloy:-

- Significant orientation effects exist in strain control specimens, manifested in a difference in strain-life of RD and TD specimens. This effect does not appear when specimens are considered on a stress-life basis. The difference is a consequence of the different stress relaxation behaviour of the two orientations, and increased modulus in the TD specimens.
- This orientation effect may be seen in notched specimens. However, the notch must be sharp enough to impose constraint on the material at the notch root, so that this material essentially experiences strain controlled deformation behaviour. If the notch is not sharp enough, the material will not show an orientation effect. This has been demonstrated by the orientation effect in V-cylindrical notch (VCN, $K_t=2.8$) specimens, which was not observed in Round-cylindrical notch (RCN, $K_t=1.4$) specimens.

- V-cylindrical notch (VCN) specimens show an extended fatigue life when compared with Round cylindrical specimens (RCN) due to a lower volume of material experiencing the peak stress applied to the specimen, and hence making VCN specimens statistically more likely to show a longer fatigue life.
- For low R ratio tests, crack initiation lives in notched specimens can be accurately predicted by empirical methods, demonstrated here by use of the Modified Coffin-Manson and Walker techniques.
- High R ratio tests in this variant of Ti6-4 are not easily predictable by the aforementioned techniques, due to the influence of additional failure mechanisms such as 'cold creep'. Ongoing research indicates that using a creep based approach may be more applicable for these specimens. This type of issue is likely to be found in most near α titanium alloys, and many $\alpha+\beta$ alloys.
- Significant differences were not found for crack propagation rates in RD and TD orientations in this alloy. However, in fatigue lifing of other alloys with stronger textures, this effect should not be ignored.

6. Acknowledgements

The author would like to acknowledge funding from EPSRC during the course of this work, and also technical advice and material from TIMET, Rolls-Royce plc and Cosworth Racing.

References

1. A.W. Bowen, "Texture stability in heat treated Ti6-4 alloys", *Mater. Sci & Eng.* **29** (1977) 19-28.
2. G. Lutjering, "Influence of processing on microstructures and mechanical properties of $\alpha+\beta$ Titanium alloys", *Mat. Sci & Eng. A* **243** (1998) 32-45.
3. M. Peters, A. Gysler, G. Lutjering, "Influence of texture on fatigue properties of Ti6-4", *Metall. Trans. A* **15** (1984) 1597-1605.
4. W.J. Evans, J.P. Jones, M.T. Whittaker, "Texture effects under tension and torsion loading conditions in titanium alloys", *Int. J. Fatigue* **27** (2005) 1244-1250.
5. M.R. Bache, W.J. Evans, B. Suddell, F.R.M. Herrouin, "The effects of texture in titanium alloys for engineering components under fatigue", *Int. J. Fatigue* **23** (2001) 153-159.
6. W.J. Evans, "Optimising mechanical properties in α/β Titanium alloys", *Mat. Sci & Eng. A* **243** (1998) 89-96.
7. P.J. Hurley, M.T. Whittaker, S.J. Williams, W.J. Evans, "Prediction of fatigue initiation lives in notched Ti 6246 specimens", *Int. J. Fatigue* **30** (2008) 623-634.
8. M.T. Whittaker, P.J. Hurley, W.J. Evans, D. Flynn, "Prediction of notched specimen behaviour at ambient and high temperatures in Ti6246", *Int. J. Fatigue* **29** (2007) 1716-1725.
9. T. Smith "The development of crystallographic texture under plane strain compression in Ti-6Al-4V" PhD thesis, University of Wales Swansea, 2005.

10. BS7270, "British standard method for constant amplitude strain controlled fatigue testing", British Standards Institution (1990).
11. L.F. Coffin "The Challenge to Unify Treatment of High Temperature Fatigue" Fatigue at High Temperatures, *ASTM STP* **520**, (1973) 744-782.
12. S.S. Manson "Fatigue: a complex subject-some simple approximations" *J. Exp. Mech.* **5** (1965) 193-226.
13. H. Neuber "Theory of stress concentration for shear-strained prismatical bodies with Arbitrary Nonlinear Stress-Strain Law" Transactions ASME , *J. Appl. Mech.* **28** (1968) 544-550.
14. K. Walker "Effects of Environment and Complex Loading History on Fatigue Life" *ASTM STP* **462** (1970) 1-14.
15. M.T. Whittaker, W.J. Evans, R. Lancaster, W. Harrison, P.S. Webster "The effect of microstructure and texture on the mechanical properties of Ti6-4", *Int. J. Fatigue* **31** (2009) 2022-2030.
16. C.A. Stubbington, "Metallurgical aspects of fatigue & fracture in Titanium alloys", *AGARD conference* **185** (1976) 140-158.
17. G.K. Haritos, T. Nicholas, D.B. Lanning, "Notch size effects in HCF behaviour of Ti6-4", *Int. J. Fatigue* **21** 1999 643-652
18. W.J. Evans, D. Davies, M.T. Whittaker "Characterisation of stress concentration features in the $\alpha + \beta$ titanium alloys" *C.Tecn. Mat.* **20** (2008) 75-80.
19. W.J. Evans, M.R. Bache "Dwell-sensitive fatigue under biaxial loads in the near-alpha titanium alloy IMI685" *Int. J. Fatigue* **16** (1994) 443-452.
20. F.P.E. Dunne, D. Rugg, A. Walker "Lengthscale-dependent, elastically anisotropic, physically-based hcp crystal plasticity: Application to cold-dwell fatigue in Ti alloys", *Int. J. Plasticity* **23** (2007) 1061-1083.
21. W.J. Evans, M.R. Bache "Dwell and environmental aspects of fatigue in α/β titanium alloys", *Fatigue Behaviour of Titanium Alloys*, The Minerals, Metals and Materials Society (1999) 99-110.
22. W.J. Evans, M.R. Bache, "Fatigue under tension/torsion loading in IMI685", *Titanium '92 Science & Technology* (1993) 1765-1772.
23. M.R. Bache, W.J. Evans, "The effect of tension-torsion loading on low temperature dwell-sensitive fatigue in titanium alloys", *Multiaxial and Fatigue design, ESIS* **21** (1996) 229-242.
24. A.W. Bowen, "The influence of crystallographic orientation on fatigue crack growth in strongly textured Ti6-4", *Acta Metall. Mater.* **23** (1975) 1401-1409.
25. M. Peters, A. Gysler, G. Lutjering, "Influence of texture on fatigue properties of Ti6-4", *Metall. Trans. A* **15** (1984) 1597-1605.